P H Y S I C A L   R E V I E W   L E T T E R S

Universal Equation of State and Pseudogap in the Two-Dimensional Fermi Gas

Marianne Bauer,[1,*] Meera M. Parish,[2] and Tilman Enss[3]
[1]*Cavendish Laboratory, Cambridge CB3 0HE, United Kingdom*
[2]*London Centre for Nanotechnology, Gordon Street, London WC1H 0AH, United Kingdom*
[3]*Institut für Theoretische Physik, Universität Heidelberg, 69120 Heidelberg, Germany*
(Received 7 November 2013; revised manuscript received 13 February 2014; published 2 April 2014)

We determine the thermodynamic properties and the spectral function for a homogeneous two-dimensional Fermi gas in the normal state using the Luttinger-Ward, or self-consistent T-matrix, approach. The density equation of state deviates strongly from that of the ideal Fermi gas even for moderate interactions, and our calculations suggest that temperature has a pronounced effect on the pressure in the crossover from weak to strong coupling, consistent with recent experiments. We also compute the superfluid transition temperature for a finite system in the crossover region. There is a pronounced pseudogap regime above the transition temperature: the spectral function shows a Bogoliubov-like dispersion with backbending, and the density of states is significantly suppressed near the chemical potential. The contact density at low temperatures increases with interaction and compares well with both experiment and zero-temperature Monte Carlo results.

The formation of fermion pairs and the superfluidity of such pairs are distinct but related phenomena: in weak-coupling BCS theory, both are predicted to occur at the same temperature T_c. However, a basic question of many-body physics is how they are related at stronger coupling and in low dimensions, where quantum fluctuations play a large role. While preformed pairs in the normal phase trivially exist in the strong-coupling Bose limit where one has tightly bound dimers, it has been argued that pairing above T_c can also occur in the BCS regime. In this case, one expects a significant suppression of spectral weight at the Fermi surface even above T_c. This so-called pseudogap regime extends up to a crossover temperature $T^* > T_c$, and its spectral and thermodynamic properties deviate strongly from the predictions of Fermi-liquid theory [1]. Recently, pairing and superfluidity have been studied in ultracold atomic gases, which afford accurate control of both the interaction strength and dimensionality, and allow access to the crossover between the BCS and Bose regimes [2]. In these systems, a pseudogap can be detected through the suppression of the spin susceptibility or directly via the spectral function, which is experimentally accessible by angle-resolved photoemission spectroscopy or momentum-resolved rf spectroscopy [3,4]. The possibility of a pseudogap regime has already been investigated both experimentally and theoretically in three dimensions (3D) [3,5].

In two-dimensional (2D) Fermi gases, the pseudogap regime is expected to be much more pronounced than in 3D, and a pairing gap has recently been observed experimentally [4]. Here, we compute the spectral function for the homogeneous 2D Fermi gas in the normal phase of the BCS-Bose crossover. Indeed, we find a strong suppression of the density of states at the Fermi surface above T_c, as shown in Fig. 1. This allows us to map the extent of the pseudogap regime in the temperature-vs-coupling phase diagram (Fig. 4), and we find that it extends further than in 3D [6].

As the binding between fermions increases, the Cooper pairs evolve into a Bose gas of tightly bound molecules. Long-range fluctuations in 2D are so strong that they inhibit superfluid long-range order at nonzero temperature. Thus, the 2D Bose gas exhibits a Berezinskii-Kosterlitz-Thouless (BKT) transition at $T_c > 0$ into a quasiordered phase with algebraically decaying correlations [7–9]. It is a challenging many-body problem to precisely characterize the crossover between the bosonic BKT and fermionic BCS limits, where the composite nature of the molecules becomes apparent.

In this Letter, we present the first computation of the finite-temperature density and pressure equation of state in the crossover regime and find a strong renormalization already for moderate interactions—see Fig. 2. The pressure at low temperatures has very recently been measured in experiment [10]. We find that the pressure computed at $T \simeq 0.1T_F$ is closer to the experimental data than zero-temperature quantum Monte Carlo (QMC) calculations [11], offering a resolution of previous discrepancies (Fig. 3). Furthermore, we determine T_c for finite systems (Fig. 4), which is relevant for experiments on quasi-2D atomic gases, in the crossover regime between the known limiting cases [12]. Finally, the contact density agrees well with experiment [13] and shows surprisingly little variation with temperature (Fig. 5).

The dilute, two-component ($\uparrow$, $\downarrow$) Fermi gas with short-range interactions is described by the Hamiltonian

$$H = \sum_{\mathbf{k}\sigma}(\varepsilon_{\mathbf{k}} - \mu)c_{\mathbf{k}\sigma}^{\dagger}c_{\mathbf{k}\sigma} + \frac{g_0}{V}\sum_{\mathbf{k},\mathbf{k}',\mathbf{q}}c_{\mathbf{k}\uparrow}^{\dagger}c_{\mathbf{k}'\downarrow}^{\dagger}c_{\mathbf{k}'+\mathbf{q}\downarrow}c_{\mathbf{k}-\mathbf{q}\uparrow},$$

where $c_{\mathbf{k}\sigma}^{\dagger}$ creates a fermion with spin σ, momentum $\mathbf{k}$, and kinetic energy $\varepsilon_{\mathbf{k}} = \hbar^2\mathbf{k}^2/2m$. The chemical potential
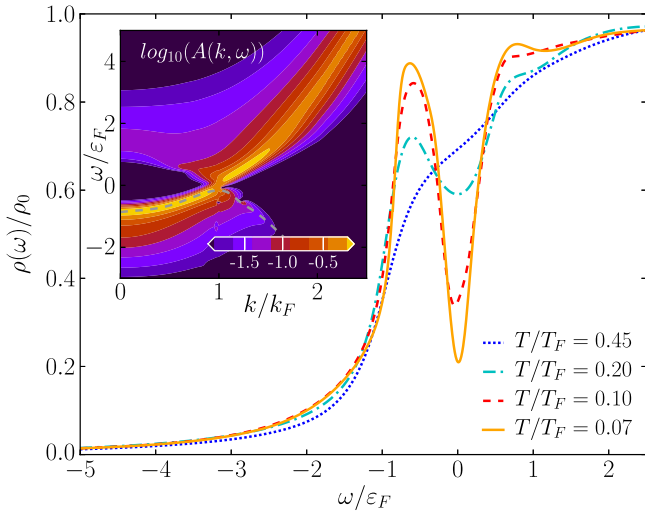
FIG. 1 (color online).   Density of states $\rho(\omega)$, normalized by $\rho_0 = m/2\pi$ for the free Fermi gas, at interaction $\ln(k_F a_{2D}) = 0.8$ for different temperatures: $T = 0.45 T_F$ (top curve at $\omega = 0$) to $T = 0.07 T_F$ (bottom). *Inset:* Spectral function $A(k,\omega)$ for $T = 0.07 T_F$. The grey dashed line marks the maximum in the spectral weight of the bottom band.

μ is taken to be the same for both species in a spin-balanced gas. The energy scale is set by the Fermi energy $\varepsilon_F = k_B T_F = \hbar^2 k_F^2/2m$ for a total density $n = k_F^2/2\pi$. The bare attractive contact interaction g_0 has to be regularized and is expressed in terms of the physical binding energy ε_B of the two-body bound state which is always present in an attractive 2D Fermi gas. We define the 2D scattering length as $a_{2D} = \hbar/\sqrt{m\varepsilon_B}$ and parametrize the interaction strength by $\ln(k_F a_{2D}) = \ln(2\varepsilon_F/\varepsilon_B)/2$. In the following, we set $k_B = 1$, $\hbar = 1$, and write $\beta = 1/k_B T$.

We investigate the behavior of the strongly interacting Fermi gas in the normal state using the Luttinger-Ward, or self-consistent T-matrix, approach [14,15], which goes beyond earlier works [6,16] by including approximately the interaction between dimers as well as dressed Green's functions. Thermodynamic precision measurements for the unitary Fermi gas in 3D [17] have confirmed the accuracy of this method, both for the value of $T_c/T_F = 0.16(1)$ and the Bertsch parameter $\xi = 0.36(1)$ [15,17]. Recently, the Luttinger-Ward approach has been extended to study transport properties [18]. The success of this method in three dimensions encourages its application to the homogeneous 2D Fermi gas, which is particularly challenging due to the logarithmic energy dependence of the scattering amplitude.

Within the Luttinger-Ward approach, pairs of dressed fermions with Green's function $G(\mathbf{k}, \omega) = [-\omega + \varepsilon_\mathbf{k} - \mu - \Sigma(\mathbf{k}, \omega)]^{-1}$ can form virtual molecules whose dynamics are described by the T matrix $\Gamma(\mathbf{K}, \Omega)$. The fermions can scatter from these molecules, which determines their lifetime and self-energy $\Sigma(\mathbf{k}, \omega)$ (see Supplemental Material [19]). From the self-consistent solution $G(\mathbf{k}, \omega)$ one obtains the spectral function $A(\mathbf{k}, \omega) = \text{Im} G(\mathbf{k}, \omega + i0)/\pi$.
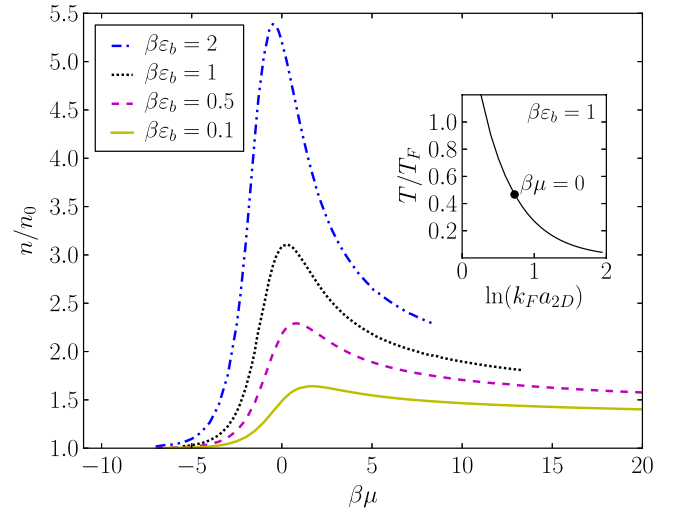

FIG. 2 (color online).   Density n of the 2D Fermi gas vs chemical potential $\beta\mu$, for different interaction strengths $\beta\varepsilon_B$ (see legend). Since the density is normalized by $n_0(\beta\mu)$ for the noninteracting gas, the nonmonotonic behavior of n/n_0 reflects the impact of interactions, while the compressibility $\kappa = (\partial n/\partial\mu)/n^2$ is always positive. The inset shows a typical trajectory in T/T_F vs $\ln(k_F a_{2D})$ corresponding to the dotted line of fixed $\beta\varepsilon_B = 1$. Along this line, $\beta\mu$ increases with decreasing T/T_F.

Density of states.—The density of states $\rho(\omega)$ describes at which energies fermionic quasiparticles can be excited, and is computed as the momentum average of the spectral function, $\rho(\omega) = \int d\mathbf{k} A(\mathbf{k}, \omega)/(2\pi)^2$. Figure 1 shows the density of states for an interaction strength of $\ln(k_F a_{2D}) = 0.8$, which is weak enough that there should be a Fermi surface at low temperatures [20]. For decreasing temperature, we see that the density of states is strongly suppressed at the chemical potential, while it increases on either side of the Fermi surface. This marks the pseudogap regime which is part of the
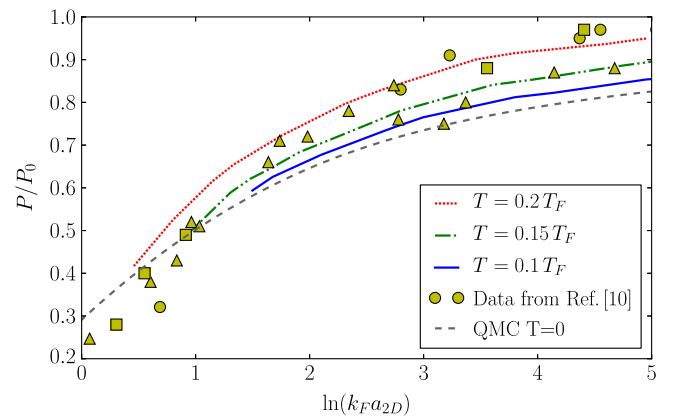

FIG. 3 (color online).   Pressure P vs interaction strength, normalized by the pressure $P_0 = n\varepsilon_F/2$ of an ideal Fermi gas of the same density at $T = 0$. Luttinger-Ward data at temperature $T/T_F = 0.2$ (top, dotted line) to $T/T_F = 0.1$ (solid line) in comparison with experimental data [10] (symbols) and $T = 0$ QMC results [11] (dashed line).
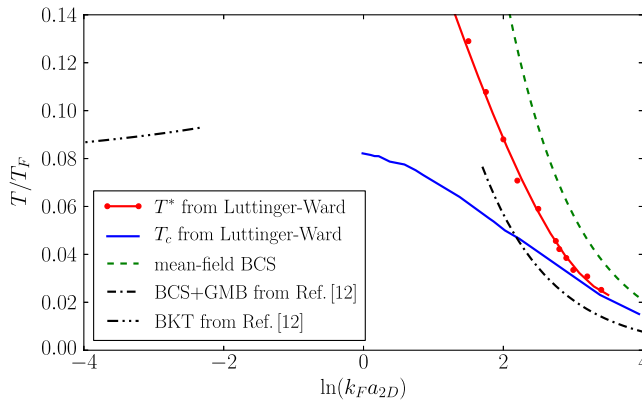
FIG. 4 (color online).   Critical temperature T_c/T_F vs interaction strength $\ln(k_F a_{2D})$. The Luttinger-Ward result for a finite system (blue solid line) in the crossover region $\ln(k_F a_{2D}) \gtrsim 0$ is compared with analytical limits [12]. The red dots mark the crossover temperature T^* to the pseudogap regime for $\ln(k_F a_{2D}) \gtrsim 1$.
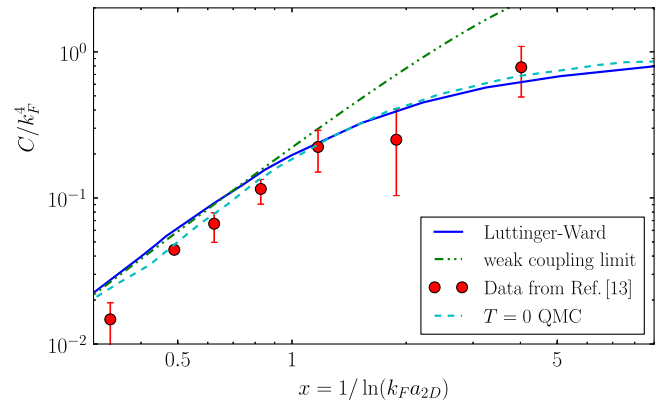

FIG. 5 (color online).   Contact density C vs interaction strength $1/\ln(k_F a_{2D})$ at temperature $T/T_F = 0.27$. We compare our result (blue solid line) with the experimental data at $T/T_F = 0.27$ [13] (red symbols), the weak-coupling result (green dashed-dotted line), and QMC calculations at $T = 0$ [11] (cyan dashed line).

normal phase, but with anomalous properties due to the lack of low-energy fermionic excitations. There is no uniquely defined temperature associated with this crossover, so for concreteness we define the pseudogap temperature T^* as the temperature where the density of states at the chemical potential drops by 25% of the value at the left fringe.

The full spectral function $A(\mathbf{k}, \omega)$, shown in the inset of Fig. 1 for a temperature of $T/T_F = 0.07$ slightly above T_c, shows a BCS-like dispersion with a clear reduction of spectral weight near the Fermi energy. While the upper branch has a minimum at a finite wave vector $k \simeq k_F$, the lower branch exhibits "backbending" towards lower energy for large momenta (cf. Ref. [6]). We note that backbending alone is not sufficient to define the pseudogap regime and can also arise for other reasons in the occupied spectral function [21]. The two-peak structure of the $k = 0$ spectral function qualitatively agrees with the momentum-resolved rf spectrum measured at $\ln(k_F a_{2D}) = 0.8$ [4], which is the only measurement that may lie within the pseudogap regime [20]. For stronger attraction, the pseudogap regime eventually crosses over into preformed fermion pairs, where the Fermi surface is lost ($\mu < 0$) and the spectral function resembles the one predicted using the virial expansion [20,22].

Density equation of state.—The total density of both spin components follows from the density of states as $n = 2 \int_{-\infty}^{\infty} d\varepsilon f(\varepsilon) \rho(\varepsilon)$, where $f(\varepsilon)$ is the Fermi distribution. In Fig. 2, we plot the density equation of state $n(\beta\mu, \beta\varepsilon_B)$ as a function of $\beta\mu$ for different values of the interaction parameter $\beta\varepsilon_B$. This manner of plotting the equation of state allows one to make a direct connection with experiments in trapped gases, since the density vs chemical potential at fixed $\beta\varepsilon_B$ can be easily extracted from the measured density profile in a trap [17]. To expose the effects of interactions, we normalize the density n by that of the ideal Fermi gas, $n_0 = 2\ln(1 + e^{\beta\mu})/\lambda_T^2$, where $\lambda_T = \sqrt{2\pi/mT}$ is the thermal wavelength. In the high-temperature limit where

$\beta\mu \rightarrow -\infty$, all properties approach those of an ideal Boltzmann gas. However, with decreasing temperature, we find that n/n_0 eventually exhibits a maximum around $\beta\mu \simeq 0$, implying that interactions are strongest at intermediate temperatures. This is easily understood from the fact that decreasing T/T_F at fixed $\beta\varepsilon_B$ results in an increasing $\ln(k_F a_{2D})$, as shown in the inset of Fig. 2. Thus, we likewise expect the system to approach a weakly interacting gas in the low temperature regime. This behavior is qualitatively different from that observed in 3D [17], and is a direct consequence of the fact that one can have a density-driven BCS-Bose crossover in 2D. The curves for large $\beta\varepsilon_B$ are shown up to the critical value $\mu_c(\beta\varepsilon_B)$ where the system is expected to enter the BKT phase.

Pressure.—The pressure is obtained by integrating the density according to the Gibbs-Duhem relation, $P(\mu)_{T, \varepsilon_B} = \int_{-\infty}^{\mu} n(\mu') d\mu'$. Figure 3 shows the Luttinger-Ward data for finite temperatures $T/T_F = 0.2$ (top) to 0.1 (bottom): the pressure decreases from the free Fermi pressure in the BCS limit to the much lower pressure of a dilute Bose gas in the BKT limit. This is a strong coupling effect beyond the mean-field BCS prediction $P = P_0$ at $T = 0$ [10,11]. As the temperature is lowered, our data approach the $T = 0$ QMC results [11] (dashed line). A recent measurement at low temperatures $T/T_F \simeq 0.04\ldots0.12$ [10] (symbols) found a deviation from the $T = 0$ pressure in the BCS limit, attributed to mesoscopic effects. We, however, find that the $T/T_F \simeq 0.1$ pressure from the Luttinger-Ward calculation agrees well with experiment in this regime, thus, suggesting that the discrepancy is in large part due to the effect of temperature.

Phase diagram of the 2D Fermi gas.—The BKT transition at a finite temperature T_c marks the onset of a nonzero superfluid density ρ_s and algebraically decaying correlations [7,8]. The jump in ρ_s/n at T_c is universal for a Bose superfluid and becomes exponentially small of order T_c/T_F on the weak-coupling BCS side [23]. The transition

temperature is characterized by the Thouless criterion, where the coefficient of the quadratic term in a Ginzburg-Landau action for the pairing field changes sign. In practice, the relevant question is when this transition occurs for a finite system, for instance inside a trapping potential (see Supplemental Material [19]). In our analysis, therefore, we compute T_c for $N = 500$ particles typical of current experiments [10], as depicted in Fig. 4. We have checked that different values for N lead to small quantitative but not qualitative changes in the T_c curve.

In the weak-coupling BCS limit $\ln(k_F a_{2D}) \gg 1$ $[\varepsilon_B \ll \varepsilon_F]$, the mean-field transition temperature is given by $T_c/T_F = (2e^{\gamma_E}/\pi) \exp[-\ln(k_F a_{2D})]$ (dashed line in Fig. 4), where $\gamma_E \approx 0.5772$ is Euler's constant [24]. Petrov *et al,* [12] have included Gor'kov–Melik-Barkhudarov (GMB) corrections and obtained a lower value $T_c/T_F = (2e^{\gamma_E}/\pi e) \times \exp[-\ln(k_F a_{2D})]$ (dashed-dotted line). On the BKT side for strong binding $\varepsilon_B \gg \varepsilon_F$, the Thouless criterion fixes $\mu_c = -\varepsilon_B/2$ and the number equation determines T_c [25]. A more elaborate analysis using Monte Carlo data for the weakly interacting Bose gas in 2D [8] yields a BKT temperature of $T_c/T_F \lesssim 0.12$ for $\ln(k_F a_{2D}) < 0$ [12], which decreases for even stronger binding (left dashed curve in Fig. 4). This limiting behavior implies the existence of a maximum T_c in the crossover region (cf. Ref. [26]), but does not determine its value or the precise crossover behavior.

The Luttinger-Ward result for T_c grows monotonically from the BCS limit towards strong coupling $\ln(k_F a_{2D}) \approx 0$: it suggests a maximum T_c at negative $\ln(k_F a_{2D})$, which is unlikely to exceed $T_c/T_F \lesssim 0.1$. This is consistent with experiments which did not observe signatures of superfluidity down to $T/T_F = 0.27$ [4], but is considerably lower than a recent calculation for a harmonically trapped gas [6].

The red dots in the phase diagram in Fig. 4 mark the crossover temperature to the pseudogap regime T^*, where the density of states $\rho(\omega)$ at the chemical potential drops by 25% of the value at the left fringe. In the weak coupling BCS limit, T^* approaches T_c since pairing and condensation occur simultaneously, and both T_c and T^* tend towards the dashed weak-coupling result. The large pseudogap regime at strong binding leads to clear signatures in the spin susceptibility and spectral properties well within reach of current experiments.

Contact density.—The contact density C [27] characterizes the probability of finding particles of opposite spin close to each other [28]. It determines the universal high-energy properties of a quantum gas with contact interactions, e.g., the momentum distribution function $n_k \to C/k^4$ at large momenta. The contact density is related to the variation of the pressure with scattering length by the adiabatic theorem [20,29]

$$C = -2\pi m \frac{dP}{d \ln a_{2D}}\bigg|_{\mu,T,V}.$$

Using the weak-coupling expansion of the ground state energy in $x = 1/\ln(k_F a_{2D})$ [30] one obtains at $T = 0$: $C = k_F^4[x^2 - (3/2 - 2\ln 2)x^3]/4$. In the normal state, the contact density corresponds to the total density of dimers [31].

In Fig. 5, we show our result for the contact (solid line) at $T = 0.27 T_F$ and compare with the experimental data at the same temperature from Fröhlich *et al.* [13], as well as with the weak-coupling estimate above. Remarkably, our calculation in this low-temperature region is very close to the $T = 0$ QMC result [11] (dashed line), showing that the contact has only a weak temperature dependence. Note, further, that while one generally expects the contact to decrease with increasing temperature, our result for larger $\ln(k_F a_{2D})$ is higher than the contact at $T = 0$ from QMC calculations, thus, suggesting that C is a nonmonotonic function of T, similar to 3D [32].

In conclusion, we have presented results for the density and pressure equation of state which shed light on a recent pressure measurement [10]. The values for the transition temperature T_c and the pseudogap crossover temperature T^* in the phase diagram reveal a large pseudogap regime; its effect on the spectral function and low-energy density of states are accessible and relevant for current experiments using momentum-resolved rf spectroscopy [4]. We find that the contact depends only weakly on temperature, providing a robust interaction gauge. It will be worthwhile to extend the Luttinger-Ward technique into the low-temperature BKT phase, which is characterized by the binding of vortex-antivortex pairs, and study the signatures of the superfluid phase for a trapped 2D Fermi gas. The BKT transition itself is revealed by a jump in the sound velocities [33].

[1] M. Randeria, in *Proceedings of the International School of Physics "Enrico Fermi" Course CXXXVI on High Temperature Superconductors* (IOS Press, Amsterdam, 1998), pp. 53–75; V. M. Loktev, R. M. Quick, and S. G. Sharapov, Phys. Rep. **349**, 1 (2001).

[2] I. Bloch, J. Dalibard, and W. Zwerger, Rev. Mod. Phys. **80**, 885 (2008); *The BCS–BEC Crossover and the Unitary Fermi Gas*, edited by W. Zwerger, Lecture Notes in Physics Vol. 836 (Springer, Berlin, 2012).

[3] J. T. Stewart, J. P. Gaebler, and D. S. Jin, Nature (London) **454**, 744 (2008); J. P. Gaebler, J. T. Stewart, T. E. Drake,

D. S. Jin, A. Perali, P. Pieri, and G. C. Strinati, Nat. Phys. **6**, 569 (2010).

[4] M. Feld, B. Fröhlich, E. Vogt, M. Koschorreck, and M. Köhl, Nature (London) **480**, 75 (2011).

[5] Q. Chen, J. Stajic, S. N. Tan, and K. Levin, Phys. Rep. **412**, 1 (2005); Y. He, Q. Chen, and K. Levin, Phys. Rev. A **72**, 011602 (2005); Q. Chen, C. A. Regal, M. Greiner, D. S. Jin, and K. Levin, Phys. Rev. A **73**, 041601 (2006); A. Perali, F. Palestini, P. Pieri, G. C. Strinati, J. T. Stewart, J. P. Gaebler, T. E. Drake, and D. S. Jin, Phys. Rev. Lett. **106**, 060402 (2011).

[6] R. Watanabe, S. Tsuchiya, and Y. Ohashi, Phys. Rev. A **88**, 013637 (2013).

[7] D. S. Fisher and P. C. Hohenberg, Phys. Rev. B **37**, 4936 (1988); Z. Hadzibabic, P. Krüger, M. Cheneau, B. Battelier, and J. Dalibard, Nature (London) **441**, 1118 (2006).

[8] N. Prokof'ev and B. Svistunov, Phys. Rev. A **66**, 043608 (2002).

[9] M. Holzmann, G. Baym, J.-P. Blaizot, and F. Laloë, Proc. Natl. Acad. Sci. U.S.A. **104**, 1476 (2007).

[10] V. Makhalov, K. Martiyanov, and A. Turlapov, Phys. Rev. Lett. **112**, 045301 (2014).

[11] G. Bertaina and S. Giorgini, Phys. Rev. Lett. **106**, 110403 (2011).

[12] D. S. Petrov, M. A. Baranov, and G. V. Shlyapnikov, Phys. Rev. A **67**, 031601 (2003).

[13] B. Fröhlich, M. Feld, E. Vogt, M. Koschorreck, M. Köhl, C. Berthod, and T. Giamarchi, Phys. Rev. Lett. **109**, 130403 (2012).

[14] R. Haussmann, Z. Phys. B **91**, 291 (1993); Phys. Rev. B **49**, 12975 (1994).

[15] R. Haussmann, W. Rantner, S. Cerrito, and W. Zwerger, Phys. Rev. A **75**, 023610 (2007).

[16] P. Nozières and S. Schmitt-Rink, J. Low Temp. Phys. **59**, 195 (1985); S. Schmitt-Rink, C. M. Varma, and A. E. Ruckenstein, Phys. Rev. Lett. **63**, 445 (1989); M. Randeria, J.-M. Duan, and L.-Y. Shieh, Phys. Rev. Lett. **62**, 981 (1989).

[17] M. J. H. Ku, A. T. Sommer, L. W. Cheuk, and M. W. Zwierlein, Science **335**, 563 (2012).

[18] T. Enss, R. Haussmann, and W. Zwerger, Ann. Phys. (N.Y.) **326**, 770 (2011); T. Enss and R. Haussmann, Phys. Rev. Lett. **109**, 195303 (2012).

[19] See Supplemental Material at http://link.aps.org/supplemental/10.1103/PhysRevLett.112.135302 for a description of the Luttinger-Ward approach, alternative definitions of a_{2D}, and the Thouless criterion for finite systems.

[20] V. Ngampruetikorn, J. Levinsen, and M. M. Parish, Phys. Rev. Lett. **111**, 265301 (2013).

[21] W. Schneider and M. Randeria, Phys. Rev. A **81**, 021601(R) (2010).

[22] M. Barth and J. Hofmann, Phys. Rev. A **89**, 013614 (2014).

[23] S. Stintzing and W. Zwerger, Phys. Rev. B **56**, 9004 (1997).

[24] K. Miyake, Prog. Theor. Phys. **69**, 1794 (1983).

[25] C. A. R. Sá de Melo, M. Randeria, and J. R. Engelbrecht, Phys. Rev. Lett. **71**, 3202 (1993).

[26] M. Drechsler and W. Zwerger, Ann. Phys. (Berlin) **504**, 15 (1992).

[27] S. Tan, Ann. Phys. (N.Y.) **323**, 2952 (2008); C. Langmack, M. Barth, W. Zwerger, and E. Braaten, Phys. Rev. Lett. **108**, 060402 (2012).

[28] E. Braaten and L. Platter, Phys. Rev. Lett. **100**, 205301 (2008).

[29] S. Tan, Ann. Phys. (N.Y.) **323**, 2971 (2008); F. Werner and Y. Castin, Phys. Rev. A **86**, 013626 (2012).

[30] P. Bloom, Phys. Rev. B **12**, 125 (1975); J. R. Engelbrecht, M. Randeria, and L. Zhang, Phys. Rev. B **45**, 10135 (1992).

[31] R. Haussmann, M. Punk, and W. Zwerger, Phys. Rev. A **80**, 063612 (2009); R. Combescot, F. Alzetto, and X. Leyronas, Phys. Rev. A **79**, 053640 (2009); Y. Nishida, Phys. Rev. A **85**, 053643 (2012).

[32] Z. Yu, G. M. Bruun, and G. Baym, Phys. Rev. A **80**, 023615 (2009).

[33] T. Ozawa and S. Stringari, Phys. Rev. Lett. **112**, 025302 (2014).